PDE6C: Novel Mutations, Atypical Phenotype, and Differences Among Children and Adults

Malena Daich Varela, Ehsan Ullah, Sairah Yousaf, Brian P. Brooks, Robert B. Hufnagel, and Laryssa A. Huryn

Ophthalmic Genetics and Visual Function Branch, National Eye Institute, National Institutes of Health, Bethesda, Maryland, United States

Correspondence: Laryssa A. Huryn, 10 Center Drive, Bldg 10, 10D45, Bethesda, MD 20892, Maryland, USA;
laryssa.huryn@nih.gov.
Robert B. Hufnagel, 10 Center Drive, Bldg 10, 10N109, Bethesda, MD 20892, Maryland, USA;
robert.hufnagel@nih.gov.

RBH and LAH are senior co-authors.

Received: May 15, 2020
Accepted: September 2, 2020
Published: October 1, 2020

Citation: Daich Varela M, Ullah E, Yousaf S, Brooks BP, Hufnagel RB, Huryn LA. PDE6C: Novel mutations, atypical phenotype, and differences among children and adults. *Invest Ophthalmol Vis Sci.* 2020;61(12):1. https://doi.org/10.1167/iovs.61.12.1

Purpose. Genetic variation in *PDE6C* is associated with achromatopsia and cone dystrophy, with only a few reports of cone–rod dystrophy in the literature. We describe two pediatric and two adult patients with *PDE6C* related cone and cone–rod dystrophy and the first longitudinal data of a pediatric patient with *PDE6C*-related cone dystrophy.

Methods. This cohort of four patients underwent comprehensive ophthalmologic evaluation at the National Eye Institute's Ophthalmic Genetics clinic, including visual field testing, retinal imaging and electroretinogram (ERG). Next-generation sequencing–based genetic testing was performed and subsequent analysis of the variants was done through three-dimensional protein models generated by Phyre2 and Chimera.

Results. All cases shared decreased best-corrected visual acuity and poor color discrimination. Three of the four patients had a cone–rod dystrophy, presenting with an ERG showing decreased amplitude on both photopic and scotopic waveforms and a mild to moderately constricted visual field. One of the children was diagnosed with cone dystrophy, having a preserved peripheral field. The children had none to minor structural retinal changes, whereas the adults had clear macular dystrophy.

Conclusions. *PDE6C*-related cone–rod dystrophy consists of a severe phenotype characterized by early-onset nystagmus, decreased best-corrected visual acuity, poor color discrimination, progressive constriction of the visual field, and night blindness. Our work contributes with valuable information toward understanding the visual prognosis and allelic heterogeneity of *PDE6C*-related cone and cone–rod dystrophy.

Keywords: PDE6C, cone dystrophy, cone–rod dystrophy, achromatopsia, phenotype

Phosphodiesterase 6 (*PDE6*) corresponds with 1 of 21 human family members of 11 subfamilies responsible for regulating the intracellular concentration of cyclic nucleotides in every tissue.[1,2] PDE6 is an essential component of the phototransduction cascade, which converts light to electrical signals within the neural retina.[3] When light activates this enzyme, intracellular cGMP is hydrolyzed, leading to a change in membrane potential and propagation of the visual cycle.[4] Rods have a PDE6 catalytic core composed of a heterodimer of PDE6A and PDE6B subunits (inhibited by PDE6G), whereas cones have a catalytic homodimer of PDE6C (inhibited by PDE6H subunits).[5] This explains why mutations in *PDE6A* (OMIM #180071), *PDE6B* (OMIM #180072) and *PDE6G* (OMIM #180073) cause autosomal recessive retinitis pigmentosa and autosomal dominant congenital stationary night blindness (both rod-related diseases),[6,7] whereas homozygous or compound heterozygous mutations in *PDE6C* and *PDE6H* (OMIM #600827 and #601190) lead to predominantly cone dysfunction disorders, such as achromatopsia (ACHM) and autosomal recessive cone dystrophy.[8,9]

Cone dystrophies are characterized by nystagmus, decreased best-corrected visual acuity (BCVA) and poor color vision. Among this group, ACHM is also described as congenital, and largely stationary lack of color discrimination.[10] About 73% ($n = 50$) of the *PDE6C* reported mutations ($n = 68$)[8,11–32] are associated with cone dystrophy ($n = 03$) and ACHM ($n = 47$), accounting for 1.0% to 2.4% of all ACHM cases.[13,33] An atypical phenotype reported in recent years with fewer *PDE6C* mutations (approximately 15%; $n = 10$)[13–17] is cone–rod dystrophy. This diagnosis not only implies decreased BCVA and color discrimination, but also progressive visual field constriction, night blindness, and decreased scotopic responses in the ERG.[34] *PDE6C* has been screened in cone–rod dystrophy cohorts and has been attributed to up to 1.8% of cases.[16,35,36] The remaining 12% ($n = 8$) of the mutations were reported to be associated with nonspecified retinal dystrophies ($n = 5$)[17,19,22,26,31] and nonretinal diseases ($n = 3$).[37–39]

In the present series, we report four unrelated individuals with mutations in *PDE6C*. The two adults and one of the children presented with cone–rod dystrophy, ascertained by ERG and visual field.

Methods

Clinical Evaluation

Patients were evaluated at the National Eye Institute, National Institutes of Health (Bethesda, MD). They were consented to an National Eye Institute–sponsored, institutional review board–approved clinical research protocol for studying the genetics of inherited eye diseases. All study protocols adhered to the tenets of the Declaration of Helsinki and complied with the Health Insurance Portability and Accountability Act. Four unrelated cases that came for evaluation owing to decreased visual acuity, nystagmus, and poor color discrimination, were found to share the same affected gene (*PDE6C*) and similar ocular phenotype.

A complete ophthalmic evaluation was performed, including measurement of BCVA, motility and alignment examination, slit lamp, and dilated fundus evaluation. Additional testing included color, red-free, and autofluorescence retinal imaging (Optos ultrawide-field retinal imaging device, Dunfermline, Scotland), Cirrus optical coherence tomography (OCT; Carl Zeiss Meditec AG, Dublin, CA), and manual Goldmann kinetic perimetry (Goldmann perimeter, Haag-Streit AG, Koniz, Switzerland). The Low Vision Cambridge Color Testing device (LvCCT; Cambridge Research Systems Ltd., Cambridge, UK) was used to test color discrimination.

ERG was performed in patients who could cooperate with testing. The International Society for Clinical Electrophysiology of Vision standard full-field ERGs were recorded using a commercial electrophysiology system (LKC, Gaithersburg, MD).[40,41] The amplitude and implicit time of both scotopic (dark adapted, 0.01; dark adapted, 3.0; and dark adapted, 10.0) and photopic (light adapted 3.0 and 30 Hz cone flicker) responses were recorded and compared with reference values to evaluate rod and cone function. A summary of the clinical characteristics of the probands affected with *PDE6C* variants can be found in Table 1.

Molecular Genetics Study

Genomic DNA was extracted from each patient's blood and different next-generation sequencing–based genetic diagnostic tests (including Sanger confirmation and segregation analysis) were performed at the CLIA-certified laboratory Blueprint Genetics. Patients A and B were tested for mutations in the achromatopsia panel, consisting of six genes (*ATF6, CNGA3, CNGB3, GNAT2, PDE6C*, and *PDE6H*). Patients C and D underwent next-generation sequencing–based retinal dystrophy panel testing, which involved 325 genes, including those in the achromatopsia panel. Pathogenic and likely pathogenic variants were further confirmed by bidirectional Sanger sequencing. Copy number variations (deletions and duplications) were also screened in patients C and D using a quantitative PCR assay. After Sanger validation and segregation analysis when parental samples were available, the American College of Medical Genetics guidelines were used to classify the variants for pathogenicity.[42] In silico predictions were obtained from VarSome (https://varsome.com/).[43] Three-dimensional protein models were generated by Phyre2 and Chimera was used to visualize the structure. Clustal omega was used to make multiple sequence alignment of PDE6C orthologous proteins.

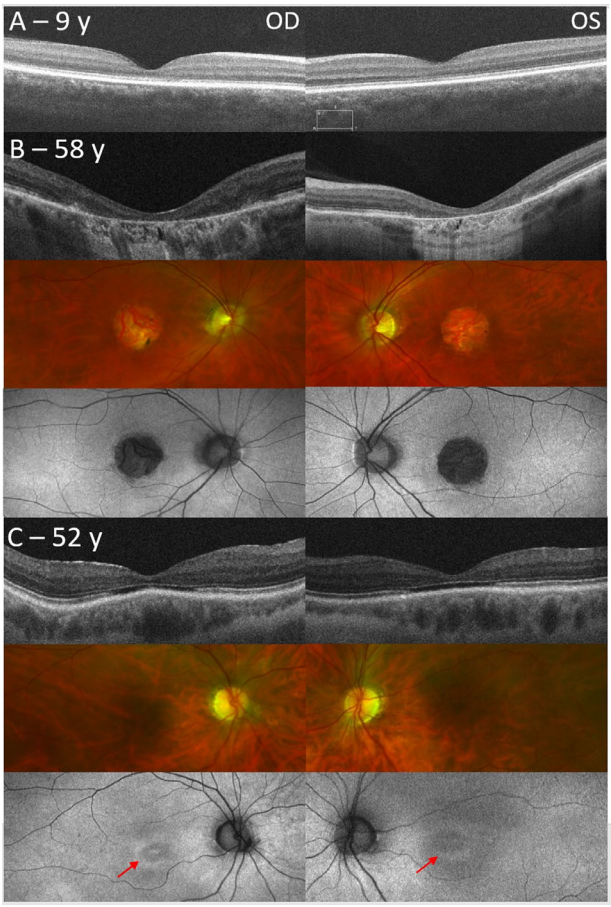

Figure 1. Cirrus OCT and Optos imagining of patients A, C, and D. (**A**) Macular OCT of patient A, showing normal foveal contour and thickness, yet mildly thinned and "ratty" outer retinal layers. (**B**) Severe macular atrophy and thinning on patient C. The atrophy is such that we are able to see the choroidal vessels both in color and autofluorescence imaging. (**C**) Symmetric subfoveal area of lucency affecting the outer layers on patient D. Blunted foveal reflex on color imaging, with a corresponding hypoautofluorescent foveal ring (marked by *red arrows* OU).

Results

Ophthalmic Findings

Patient A is a 9-year-old Latina girl who was referred for evaluation of decreased visual acuity and poor color discrimination. These symptoms were present and stable since early childhood, per report. Her BCVA was 20/200 OD and 20/250 OS, with correction of mild myopia. Motility examination showed alternating exotropia and low amplitude, moderate frequency nystagmus. Fundoscopy and red-free fundus imaging were normal. OCT revealed a central foveal thickness of 181 µm in her right eye and 184 µm in her left eye, which is within the normal range for age-based Cirrus measurements.[44] Foveal morphology was normal, although the outer retinal layers were mildly thinned (Fig. 1A). Goldmann visual field was constricted in both eyes, with a horizontal field of 80° OD and 110° OS for the V4e stimulus. There were also functional central scotomas, represented by a constricted field for the I4e isopter (Supplementary Fig. 1). The LvCCT showed no color discrimination in tritan, deutan, and protan axes, symmetric in both eyes. ERG

Table 1. Clinical Characteristics of Probands Affected With *PDE6C* Variants

Subject IDs	Sex	Age (y)	BCVA		Macular Clinical Findings (OU)	Macular OCT Characteristics (OU)	ERG		Visual Field, Continuous Horizontal Degrees (V4e Isopter)
			OD	OS			Scotopic- 0 dB Stimulus	Photopic- Cone Flicker	
Patient A	F	9	20/200	20/250	Normal	Normal	a-wave: 93 µV amplitude,* 18.25 ms implicit time; b-wave: 251.5 µV amplitude,* 51.5 ms implicit time	13 µV amplitude,* 31.5ms implicit time	80 OD and 110 OS
Patient B	M	8	20/125	20/160	Mildly blunted foveal reflex	Discontinuity of outer retinal layers	NA	NA	NA
Patient C	M	58	20/200	20/250	Atrophy	Severe retinal atrophy	a-wave: 88.5 µV amplitude,* 22.25 ms implicit time; b-wave: 153.5 µV amplitude,* 67.0 ms implicit time**	Essentially extinguished	110 OD and OS
Patient D	F	52	20/200	20/125	Blunted foveal reflex	Hypolucent area in ellipsoid zone	a-wave: 65.5 µV amplitude,* 19.25 ms implicit time; b-wave: 143.0 µV amplitude,* 54.25 ms implicit time	Essentially extinguished	110 OD and OS

NA, not available; Scotopic ERG, responses represent average a-wave and b-wave amplitudes and average implicit times to the 0 dB stimulus; Photopic ERG, 30 Hz cone flicker average amplitude and average implicit times.

* Reduced amplitudes.

** Delayed implicit times.

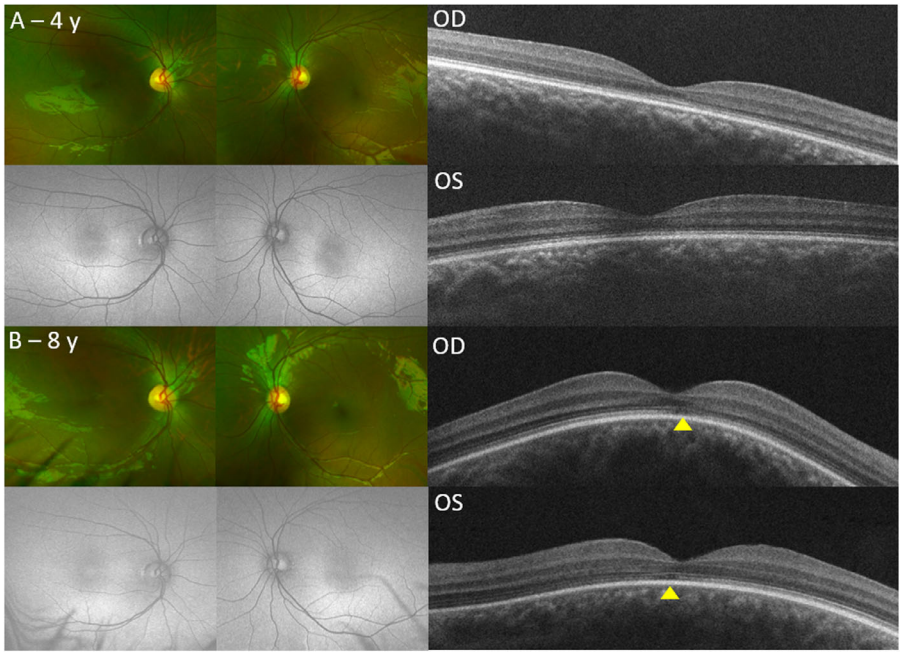

Figure 2. Patient's B longitudinal evaluation. (**A**) corresponds to his first visit at age 4 in which the macular outer retinal layers were continuous and both color and autofluorescence imaging showed no abnormalities. (**B**) are images at age 8, in which discontinuity of the outer layers was noted, nasal to the fovea (marked with *yellow arrowheads*). Both OCT line scans are located within the macula, but alignment is unavailable owing to poor fixation. Color and autofluorescence show none to subtle changes.

photopic responses were severely diminished, and scotopic responses were moderately diminished with normal implicit times (Table 1).

Patient B is an 8-year-old Asian boy who was referred for nystagmus. He described having issues with color vision, glare, and bright lights. His parents did not note changes in his visual function over time. He was 4 years old on his first visit and he has had 4 yearly follow-up visits (Fig. 2A). On his most recent visit (8 years of age), ophthalmic evaluation measured a BCVA of 20/125 OD and 20/160 OS, using red-tinted lenses with mild myopia and astigmatism correction. The patient was orthophoric and presented with low-amplitude, high-frequency nystagmus. Fundus examination showed a bilateral and symmetric mildly blunted foveal reflex. Vessels and periphery were within normality. Central scotomas were noticed on confrontation visual field testing. The LvCCT showed no color discrimination in tritan, deutan, and protan axes, symmetric in both eyes. ERG could not be performed owing to young age and poor cooperation. Although visual acuity, color discrimination and fundus evaluation were stable over the 4 years of follow-up, a subtle subfoveal discontinuity of the outer retinal layers was noticed on his most recent OCT, at age 8 (Fig. 2B). This finding was present in only one cut of the OCT, symmetrically in both eyes. Yet, his central foveal thickness was still normal according to age: 164 µm OD and 162 µm OS.[44]

Patient C is a 58-year-old Caucasian man who presented for evaluation of cone–rod dystrophy. He reported nonprogressive low visual acuity from birth and absent color vision. His light sensitivity, however, had worsened in the last 10 years. His visual acuity measured 20/200 OD and 20/250 OS. The patient presented with bilateral, symmetric, low-amplitude, high-frequency nystagmus. His retinal examination showed well-circumscribed macular atrophy and nasal peripheral cobblestone atrophic areas bilaterally. His retinal vessels were mildly attenuated and the optic nerve had normal color and cupping. OCT revealed severe macular atrophy with loss of the outer retinal layers (Fig. 1B). Central foveal thickness was decreased at 109 and 102 µm in his right and left eyes, respectively. Goldmann visual field showed constricted field for the isopter I2e and temporal constriction bilaterally (110° horizontal visual field OD and OS for V4e stimulus) (Supplementary Fig. 1). The ERG showed severely decreased amplitude of photopic responses and moderate decrease of scotopic responses, with increased latency (Table 1).

Patient D is a 52-year-old Ashkenazi Jewish woman who presented with scotomas, color vision issues, and poor visual acuity since she was 16 years old. These symptoms worsened over time, she had undergone two bilateral strabismus surgeries, LASIK, and cataract surgery on both eyes. Her BCVA was 20/200 OD and 20/160 OS, with a myopic correction. She had right exotropia and end-gaze nystagmus in both eyes. Slit-lamp evaluation revealed mild corneal scarring outside the visual axis, possibly related to contact lens use. On fundus examination, the foveal reflex was absent. The retinal vessels were normal and the periphery had myopic pigmentary changes. Autofluorescence imaging revealed a mild hypoautofluorescent foveal ring in both eyes. OCT showed macular thinning with a symmetric hypolucent area affecting the foveal ellipsoid zone (Fig. 1C). Central foveal thickness was decreased: 143 and 136 µm in the right and left eyes, respectively. Goldmann visual field showed constriction of the I3e isopter with mildly constricted field for the V4e stimulus (110° OD and OS, Supplementary Fig. 1). The LvCCT showed no color discrimination in all axes (tritan, deutan, and protan). ERG revealed a flat photopic response and decreased amplitude in scotopic testing (Table 1, Fig. 3).

Investigative Ophthalmology & Visual Science

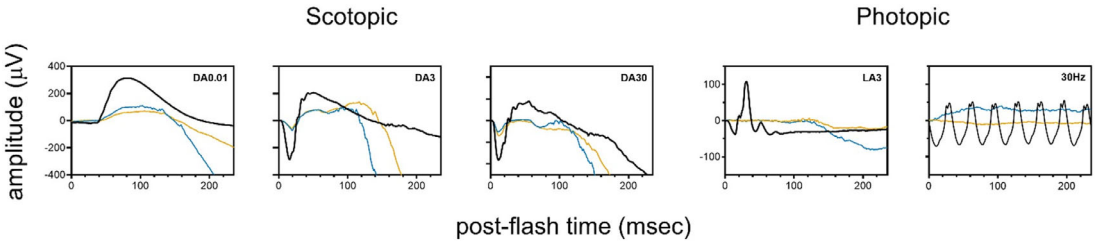

Figure 3. Full-field ERG in patient D. Black waveforms correspond to a normal responses. *Blue* and *orange* indicate OD and OS in patient D, respectively. Photopic responses are essentially extinguished and the amplitude of scotopic responses is severely decreased as well.

Table 2. Genetic Details of Our Patients' Variants

Subject IDs	Ethnicity	cDNA and Amino Acid Change	GnomAD	ACMG Classification	Predicted Pathogenic	References
Patient A	Latino	c.1579C>T, p.(Arg527*)	0.00004377	Pathogenic (PVS1, PM2, PM3, PP5)	NA	Dedania et al.[12] Weisschuh et al.[13]
		c.939+2T>G, p.?	0.00000398	Pathogenic (PVS1, PM2, PM3)	NA	This study
Patient B	Asian	c.2377C>T, p.(Arg793Trp)	0.00000399	VUS (PM2, PP3)	DANN, DEOGEN2, FATHMM-MKL, M-CAP, MVP, MutationAssessor and REVEL	This study
Patient C	Caucasian	c.1652C>T, p.(Thr551Ile)	0.00000397	VUS (PM2, PP3)	DANN, DEOGEN2, EIGEN, FATHMM-MKL, M-CAP, MVP, MutationAssessor, MutationTaster, PrimateAI, REVEL and SIFT	This study
Patient D	Ashkenazi Jewish	c.1307C>G, p.(Thr436Ser)	0.00002786	VUS (PM2, PP2)	DEOGEN2, EIGEN, M-CAP, MVP, PrimateAI, REVEL and SIFT: benign.DANN, FATHMM-MKL, MutationAssessor and MutationTaster	This study

ACMG, American College of Medical Genetics; VUS, variants of uncertain significance.

A summary of the ocular findings in our cohort is presented in Table 1.

Genetic Testing Results

In all four cases, consanguinity was denied, and the family history was negative for ocular disorders. There was no family or personal history of hearing loss, seizures, or any other syndromic features usually associated with inherited eye diseases.

A summary of the genetic findings in our cohort is described in Table 2. In patient A, we identified two heterozygous putative loss-of-function mutations in *PDE6C* gene. A previously reported nonsense mutation, NM_006204.4:c.1579C>T; p.Arg527Ter[12,13] was inherited paternally (Fig. 4A). It was located in exon 12, which corresponds with the PDEase (3'5'-cyclic nucleotide phosphodiesterase) catalytic domain (https://www.uniprot.org/uniprot/P51160#family_and_domains accessed on 05/13/2020). This mutation is listed in ClinVar as pathogenic and has an allele frequency of 0.00004377 in gnomAD (https://gnomad.broadinstitute.org/ accessed on 05/13/2020). The second variant is a novel canonical splice donor mutation c.939+2T>G that was inherited maternally, satisfying a compound heterozygous inheritance pattern. It is located downstream of exon 5 and it is affecting the splicing of the GAF2 domain. This variant is absent from ClinVar and HGMD, has an allele frequency of 0.000003985 (gnomAD) and was classified as "Pathogenic" by using the American College of Medical Genetics classification criteria described by Richards et al., 2015.[42]

Patients B, C, and D were each homozygous for novel variants of uncertain significance in *PDE6C*, according to the American College of Medical Genetics classification (Fig. 4, Table 2).[42] All three variants NM_006204.4:c.2377C>T, p.(Arg793Trp), NM_006204.4:c.1652C>T, p.(Thr551Ile), and NM_006204.4:c.1307C>G, p.(Thr436Ser) are rare in the general population (gnomAD allele frequency 0.00000399, 0.00000397, and 0.00002786, respectively) and predicted to be deleterious by in silico predictions.

It is necessary for PDE6 proteins to reach their destination in the ciliary compartment of the photoreceptors to perform their function. Variants in *PDE6C* gene may produce truncated or improperly folded proteins that might restrict its transport toward the rods' outer segments. An inappropriate amount of functional PDE6 elevates cGMP levels, resulting in rapid retinal degeneration in both humans and animal models.[45,46] The variants in the current study were

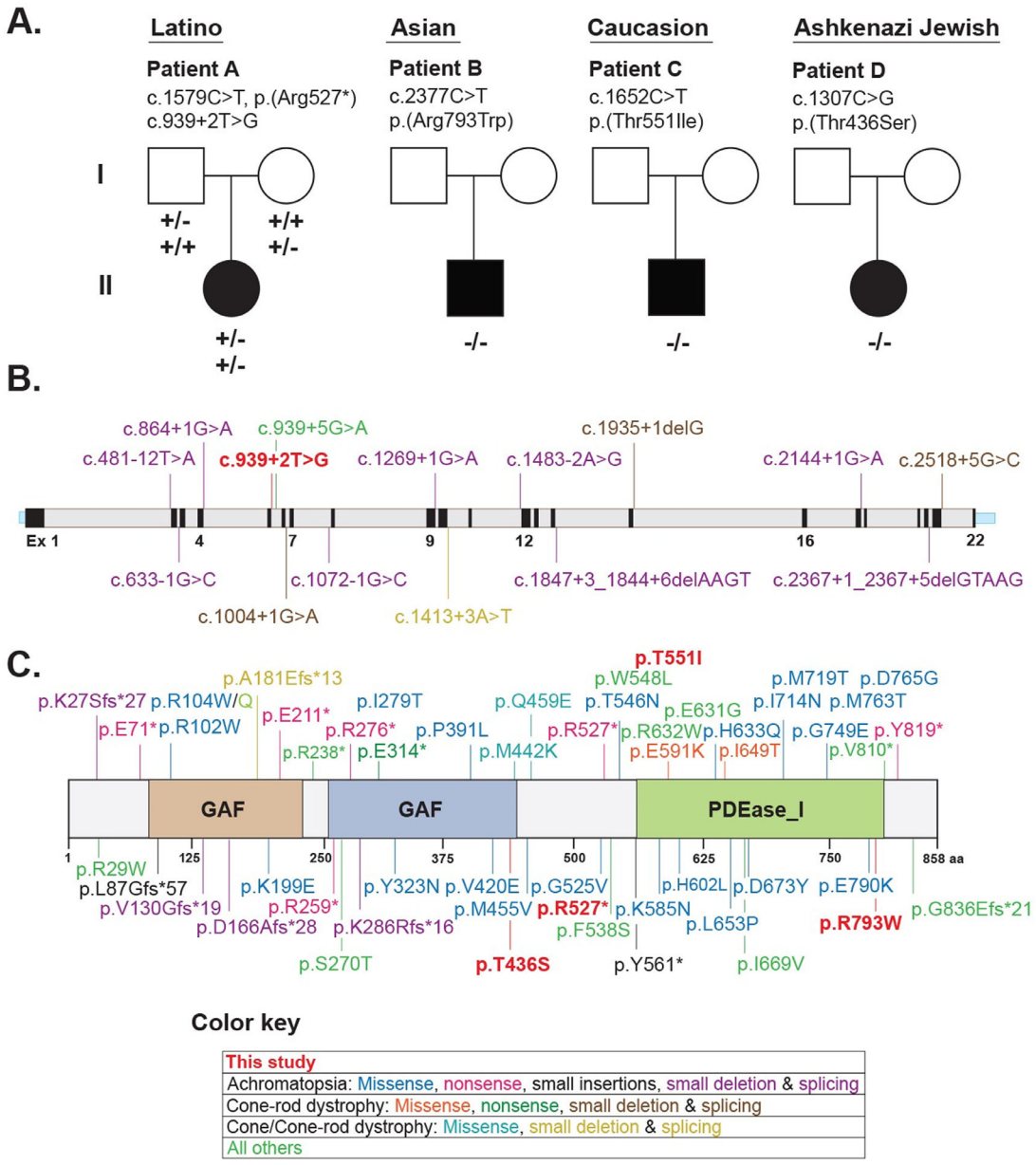

Figure 4. Probands harboring variants in *PDE6C* gene. Schematic representation PDE6C gene and protein structure with all of the reported *PDE6C* variants. (**A**) Pedigrees of probands, Filled and empty symbols represent affected and unaffected individuals respectively. (**B**) Illustration of *PDE6C* gene (NM_006204.4) with novel splicing (this study) and reported splicing/small deletion variants (HGMD). (**C**) PDE6C protein domain structure (Uniprot_P51160) with identified and reported missense, nonsense and small insertion/deletion variants. GAF (cGMP-specific phosphodiesterases) is a widespread small molecule binding domain, which helps to stabilize catalytic dimer formation. PDEase (3'5'-cyclic nucleotide phosphodiesterase) is important to regulate cAMP catabolism, a vital step in signal transduction pathway. All others represent the following disease phenotypes: autism spectrum disorder, cone dystrophy—early onset, high myopia, Leber congenital amaurosis, major depressive disorder, retinal dystrophy with early onset, and ACHM.

assessed by conservation analysis and three-dimensional protein modeling (Figs. 5 and 6). The p.Arg793Trp substitution present on patient B is located in the PDEase-I domain and is predicted to diminish intraprotein interactions with other residues (Fig. 5) owing to an increase in hydrophobic forces, which may affect protein folding. However, the missense variant found in patient B [p. (Arg793Trp)] present in catalytic domain, may fold precisely and transport properly to the rods' outer segments with reduced proteolytic stability, in accordance to similar variants (p.His602Leu and p.Glu790Lys) investigated for functional act by another group.[46] As per molecular modeling prediction, p.Thr551Ile substitution detected in patient C is proximal to the zinc ion binding site in the PDEase-I domain, which is important for enzymatic activity (Fig. 5). In the same study conducted by Cheguru et al.,[46] 2015, a nearby variant (p.Met455Val) of *PDE6C* found in patient A [p. (Arg527*)] and patient C [p.(Thr551Ile)], a nonconserved part of the protein] is reported to transport toward the outer segments, but in a diffused pattern, suggesting a disc rim locality failure. Finally, the missense variant p.Thr436 is part of the GAF B domain, found in cGMP-specific phosphodiesterases and

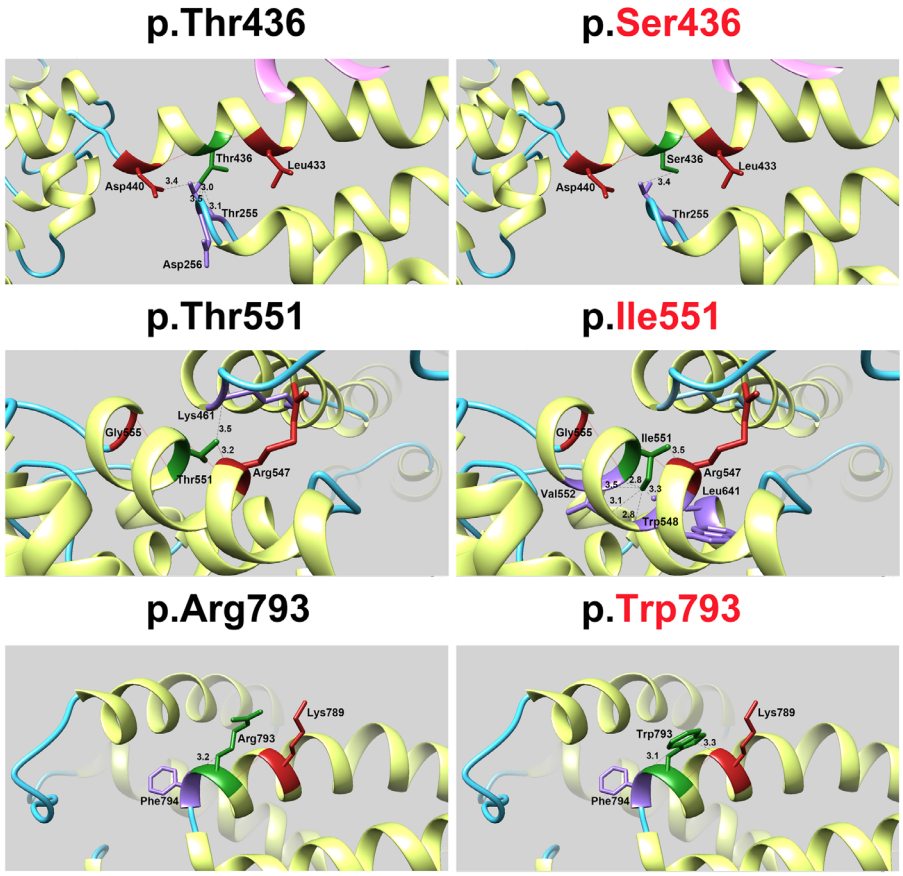

Figure 5. Protein model of PDE6C with structural modeling of PDE6C missense variants. The protein secondary structure is shown in the following colors: helix, *yellow*; strand, *pink*; and coil, *blue*. Residues of interest are shown in *forest green* color and hydrogen bonding involved residues and bonding pattern are shown in *brick red* color. *Purple* color is used to show nearby residues and their distance is drawn with *black dashed lines*.

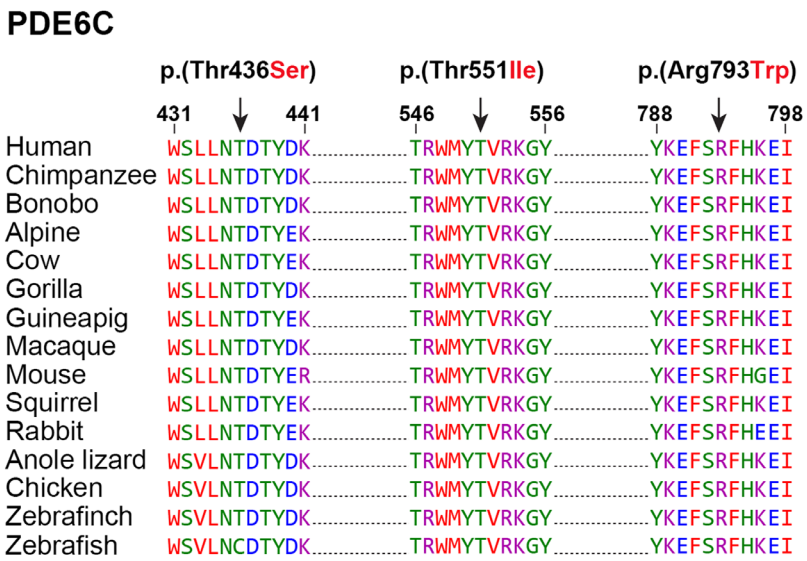

Figure 6. Clustal alignment of PDE6C missense variants. Representation of the conservation of amino acids affected by missense variants reported in this study across a number of species.

involved in binding of other molecules (Fig. 5). A missense variant (p.Pro391Leu) of *PDE6C* present in GAF B domain is reported to result in decreased PDE activity in highly significant manner.[47] In our study, [p.(Thr436Ser)] also resides in GAF B domain and might affect protein activity in a similar way.

Discussion

Achromatopsia is typically diagnosed in early childhood in patients with nystagmus, decreased BCVA, and poor color vision.[48] Parents are often concerned about the visual prognosis and progression of the disease as the child grows. The stationary course of ACHM is an ongoing topic of discussion. This disease is typically characterized as being stable throughout life, although recent papers have shown evidence of progressive cone and even rod involvement in patients with *CNGA3*,[50] *CNGB3*,[49,50] and *PDE6C* variants.[32,49] In contrast, other groups[51,52] did not find a clear correlation between age and progression of disease.

We present both children and adults, their cross-sectional data, and the longitudinal evaluation of patient B, followed regularly for 4 years. We note two discernibly different phenotypes in these groups. The children had minor to no structural retinal changes and the adults had macular dystrophy. Although macular dystrophy in adults can be certainly attributed to other common causes such as age-related macular dystrophy or traumatic maculopathy, the presence of a long-standing history of decreased visual acuity as well as the nystagmus on our adult patients led us to think that these structural changes were related with their primary condition, instead of having a superimposed one. Functionally, there were no significant differences among the two groups regarding visual acuity and color discrimination. As Sadowski and Zrenner[53] mention, a superimposed rod defect in cone dystrophies can be noticed as a constricted visual field and/or by electrophysiology. The patients who underwent electrophysiologic testing (patients A, C, and D) showed decreased photopic and scotopic responses as well as visual field constriction, allowing us to classify these phenotypes as a cone–rod dystrophy. Interestingly, these patients did not report nyctalopia and preferred mesopic conditions, owing to photophobia. Therefore, cone-derived symptoms may be predominant over the scotopic ones. The progression of the children's phenotype toward the one of the adults remains unknown and could only be answered by a large longitudinal study. The OCT abnormalities noted in patient B during follow-up evaluations support the possibility of progression; however, we are limited in our ability to confirm scan alignment owing to patient cooperation and image quality. However this longitudinal report of a pediatric patient with *PDE6C* ACHM raises questions about the progressive versus stationary course of this disease. The different phenotypes reported may be part of a continuous spectrum and we believe that as more patients are phenotyped, these questions will be answered.

All the patients in our cohort presented with novel *PDE6C* variants, three in homozygosity and one in a compound heterozygous state. In patient A, p.Arg527Ter was previously reported in patients having ACHM, decreased BCVA, and a stable examination, although no information was provided regarding age or retinal findings.[12,13] Its compound heterozygous mutation c.939+2T>G was novel, but a nearby mutation (c.940G>T, p.Glu314Ter) was reported to present with cone–rod dystrophy, although Wang et al.[14] did not disclose further details.

Our three-dimensional protein analysis of the missense mutation p.Arg793Trp (patient B) predicted a decrease in the normal function of the protein, by decreased interaction with other residues and incorrect protein folding. Functional testing in two other missense arginine to tryptophan variants (Arg29Trp and Arg104Trp) has shown highly significant decrease in PDE activity, by affecting its binding and dimerization.[11] One could speculate that the amino acid change from a positively charged arginine to a neutral tryptophan is therefore a significant modification that may, in our case, alter the function of the PDE domain. The patients reported by Grau et al.[11] (Arg29Trp and Arg104Trp) had ACHM with essentially normal macula in the fundus evaluation, nystagmus, severe color vision defects and photophobia. Only the age and OCT of the patient carrying the Arg29Trp mutation were reported: 33 years old and a subfoveal optically empty cavity in the ellipsoid zone in both eyes.

No functional testing has been reported on similar or nearby mutations of patient C's p.Thr551Ile. Adjacent variants (p.Thr546Asn and p.Trp548Leu) only mention ACHM as the phenotype of the patients, with no further information or pictures provided.[13,24]

Mutations near that of patient D's variant (p.Thr436Ser) were classified as pathogenic (e.g., p.Val402Glu, p.Met442Lys, and p.Met455Val).[8,15,22] The phenotype's description of the first two mutations is imprecise, only stating that the patients had ACHM.[15,22] The patient with p.Met455Val variant was 37 years old, had mild pigmentary macular changes, and had a hypolucent area subfoveally by OCT.[8]

As mentioned elsewhere in this article and described across the literature, a spectrum of phenotypes has been associated with *PDE6C*, ranging from ACHM and early-onset cone dystrophy to cone–rod dystrophy and macular atrophy.[8,30,32,33,49] Most patients with *PDE6C* variants exhibit ACHM and normal fundus examination or minor macular changes, even as adults.[27,28] Macular atrophy has been reported,[32,33] although this feature is more commonly seen in patients with other affected genes, such as *CNGB3*.[54] Our patients' phenotype correspond with one associated with *PDE6C*, showing poor color discrimination, decreased BCVA, nystagmus, and macular and cone–rod dystrophy. This finding, along with the specifics on every mutation (in silico tools predictions, gnomAD frequency), makes us call these variants novel disease-causing *PDE6C* mutations.

Conclusions

Our cohort provides evidence of rod involvement in patients with *PDE6C* mutations, which is an atypical presentation for this gene. Additional data and longitudinal points are needed to have accurate information regarding progression and visual prognosis, however our cohort suggests visual acuity and color discrimination may remain stable over time, whereas functional (i.e., rod involvement) changes may present over time. Given that gene therapy for ACHM is currently in the clinical trial phase, knowing when clinical findings appear could narrow the therapeutic window and therefore be a valuable information for both patients and ophthalmologists. Moreover, expanding the spectrum of *PDE6C* disease-causing mutations improves our understanding of its function and expression as well as the pathophysiology and visual prognosis of this condition.

Acknowledgments

The authors thank Brett Jeffrey, Delphine Blain, and Amy Turriff for their valuable work with our patients and assistance with this project.

Supported by the National Institutes of Health – Intramural Research Program.

Investigative Ophthalmology & Visual Science

Disclosure: **M. Daich Varela,** None; **E. Ullah,** None; **S. Yousaf,** None; **B.P. Brooks,** None; **R.B. Hufnagel,** None; **L.A. Huryn,** None

References

1. Bender AT, Beavo JA. Cyclic nucleotide phosphodiesterases: molecular regulation to clinical use. *Pharmacol Rev*. 2006;58:488–520.
2. Lagman D, Franzén IE, Eggert J, Larhammar D, Abalo XM. Evolution and expression of the phosphodiesterase 6 genes unveils vertebrate novelty to control photosensitivity. *BMC Evol Biol*. 2016;16:124, Published 2016 Jun 13, doi:10.1186/s12862-016-0695-z.
3. Arshavsky VY, Lamb TD, Pugh EN, Jr. G proteins and phototransduction. *Annu Rev Physiol*. 2002;64:153–187.
4. Cote RH. Characteristics of photoreceptor PDE (PDE6): similarities and differences to PDE5. *Int J Impot Res*. 2004;16:S28–S33.
5. Gopalakrishna KN, Boyd K, Artemyev NO. Mechanisms of mutant PDE6 proteins underlying retinal diseases. *Cell Signal*. 2017;37:74–80.
6. Mizobuchi K, Katagiri S, Hayashi T, et al. Clinical findings of end-stage retinitis pigmentosa with a homozygous *PDE6A* variant (p.R653X). *Am J Ophthalmol Case Rep*. 2018;13:110–115.
7. Palmowski-Wolfe A, Stingl K, Habibi I, et al. Novel PDE6B mutation presenting with retinitis pigmentosa – a case series of three patients. *Klin Monbl Augenheilkd*. 2019;236:562–567.
8. Thiadens AA, den Hollander AI, Roosing S, et al. Homozygosity mapping reveals PDE6C mutations in patients with early-onset cone photoreceptor disorders. *Am J Hum Genet*. 2009;85:240–247, doi:10.1016/j.ajhg.2009.06.016.
9. Kohl S, Coppieters F, Meire F, et al. A nonsense mutation in PDE6H causes autosomal-recessive incomplete achromatopsia. *Am J Hum Genet*. 2012;91:527–532, doi:10.1016/j.ajhg.2012.07.006.
10. Michaelides M, Hunt DM, Moore AT. The cone dysfunction syndromes. *Br J Ophthalmol*. 2004;88:291–297, doi:10.1136/bjo.2003.027102.
11. Grau T, Artemyev NO, Rosenberg T, et al. Decreased catalytic activity and altered activation properties of PDE6C mutants associated with autosomal recessive achromatopsia. *Human Mol Genet*. 2011;20:719–730, doi:10.1093/hmg/ddq517.
12. Dedania VS, Liu JY, Schlegel D, et al. Reliability of kinetic visual field testing in children with mutation-proven retinal dystrophies: Implications for therapeutic clinical trials. *Ophthalmic Genet*. 2018;39:22–28, doi:10.1080/13816810.2017.1329447.
13. Weisschuh N, Stingl K, Audo I, et al. Mutations in the gene *PDE6C* encoding the catalytic subunit of the cone photoreceptor phosphodiesterase in patients with achromatopsia. *Human Mutat*. 2018;39:1366–1371, doi:10.1002/humu.23606.
14. Wang P, Li S, Sun W, et al. An ophthalmic targeted exome sequencing panel as a powerful tool to identify causative mutations in patients suspected of hereditary eye diseases. *Transl Vis Sci Technol*. 2019;8:21, Published 2019 Apr 25, doi:10.1167/tvst.8.2.21.
15. Boulanger-Scemama E, El Shamieh S, Démontant V, et al. Next-generation sequencing applied to a large French cone and cone-rod dystrophy cohort: mutation spectrum and new genotype-phenotype correlation. *Orphanet J Rare Dis*. 2015;10:85, Published 2015 Jun 24, doi:10.1186/s13023-015-0300-3.
16. Huang L, Xiao X, Li S, et al. Molecular genetics of cone-rod dystrophy in Chinese patients: new data from 61 probands and mutation overview of 163 probands. *Exp Eye Res*. 2016;146:252–258, doi:10.1016/j.exer.2016.03.015.
17. Patel N, Aldahmesh MA, Alkuraya H, et al. Expanding the clinical, allelic, and locus heterogeneity of retinal dystrophies. *Genet Med*. 2016;18:554–562, doi:10.1038/gim.2015.127.
18. Carss KJ, Arno G, Erwood M, et al. Comprehensive rare variant analysis via whole-genome sequencing to determine the molecular pathology of inherited retinal disease. *Am J Hum Genet*. 2017;100:75–90, doi:10.1016/j.ajhg.2016.12.003.
19. Abouelhoda M, Sobahy T, El-Kalioby M, et al. Clinical genomics can facilitate countrywide estimation of autosomal recessive disease burden. *Genet Med*. 2016;18:1244–1249, doi:10.1038/gim.2016.37.
20. Chang B, Grau T, Dangel S, et al. A homologous genetic basis of the murine cpfl1 mutant and human achromatopsia linked to mutations in the PDE6C gene. *Proc Natl Acad Sci USA*. 2009;106:19581–19586, doi:10.1073/pnas.0907720106.
21. Xiong HY, Alipanahi B, Lee LJ, et al. RNA splicing. The human splicing code reveals new insights into the genetic determinants of disease. *Science*. 2015;347:1254806, doi:10.1126/science.1254806.
22. Weisschuh N, Mayer AK, Strom TM, et al. Mutation detection in patients with retinal dystrophies using targeted next generation sequencing. *PLoS One*. 2016;11:e0145951, Published 2016 Jan 14, doi:10.1371/journal.pone.0145951.
23. Riera M, Navarro R, Ruiz-Nogales S, et al. Whole exome sequencing using Ion Proton system enables reliable genetic diagnosis of inherited retinal dystrophies. *Sci Rep*. 2017;7:42078, Published 2017 Feb 9, doi:10.1038/srep42078.
24. Kim MS, Joo K, Seong MW, et al. Genetic mutation profiles in Korean patients with inherited retinal diseases [published correction appears in J Korean Med Sci. 2019 Sep 09;34(35):e245]. *J Korean Med Sci*. 2019;34:e161, Published 2019 Jun 2, doi:10.3346/jkms.2019.34.e161.
25. Langlo CS, Patterson EJ, Higgins BP, et al. Residual foveal cone structure in CNGB3-associated achromatopsia. *Invest Ophthalmol Vis Sci*. 2016;57:3984–3995, doi:10.1167/iovs.16-19313.
26. Ellingford JM, Barton S, Bhaskar S, et al. Molecular findings from 537 individuals with inherited retinal disease. *J Med Genet*. 2016;53:761–767, doi:10.1136/jmedgenet-2016-103837.
27. Abdelkader E, Brandau O, Bergmann C, AlSalamah N, Nowilaty S, Schatz P. Novel causative variants in patients with achromatopsia. *Ophthalmic Genet*. 2018;39:678–683, doi:10.1080/13816810.2018.1522653.
28. Lee H, Deignan JL, Dorrani N, et al. Clinical exome sequencing for genetic identification of rare Mendelian disorders. *JAMA*. 2014;312:1880–1887, doi:10.1001/jama.2014.14604.
29. Di Iorio V, Karali M, Brunetti-Pierri R, et al. Clinical and genetic evaluation of a cohort of pediatric patients with severe inherited retinal dystrophies. *Genes (Basel)*. 2017;8:280, Published 2017 Oct 20, doi:10.3390/genes8100280.
30. Huang L, Zhang Q, Li S, et al. Exome sequencing of 47 Chinese families with cone-rod dystrophy: mutations in 25 known causative genes. *PLoS One*. 2013;8:e65546, Published 2013 Jun 11, doi:10.1371/journal.pone.0065546.
31. Porto FBO, Jones EM, Branch J, et al. Molecular screening of 43 Brazilian families diagnosed with Leber congenital amaurosis or early-onset severe retinal dystrophy. *Genes (Basel)*. 2017;8:355, Published 2017 Nov 29, doi:10.3390/genes8120355.

32. Georgiou M, Robson AG, Singh N, et al. Deep phenotyping of PDE6C-associated achromatopsia. *Invest Ophthalmol Vis Sci*. 2019;60:5112–5123, doi:10.1167/iovs.19-27761.
33. Katagiri S, Hayashi T, Yoshitake Ket al. Congenital achromatopsia and macular atrophy caused by a novel recessive *PDE6C* mutation (p.E591K), *Ophthalmic Genetics*. 2015;36:137–144
34. Hamel CP. Cone rod dystrophies. *Orphanet J Rare Dis*. 2007;2:7, Published 2007 Feb 1, doi:10.1186/1750-1172-2-7.
35. Huang L, Li S, Xiao X, Jia X, Wang P, Guo X, Zhang Q. Screening for variants in 20 genes in 130 unrelated patients with cone-rod dystrophy. *Mol Med Rep*. 2013;7.6:1779–1785.
36. Birtel J., Eisenberger T., Gliem M, et al. Clinical and genetic characteristics of 251 consecutive patients with macular and cone/cone-rod dystrophy. *Sci Rep*. 2018;8:4824, https://doi.org/10.1038/s41598-018-22096-0.
37. Wong ML, Dong C, Andreev V, Arcos-Burgos M, Licinio J. Prediction of susceptibility to major depression by a model of interactions of multiple functional genetic variants and environmental factors. *Mol Psychiatry*. 2012;17:624–633, doi:10.1038/mp.2012.13.
38. Iossifov I, O'Roak BJ, Sanders SJ, et al. The contribution of de novo coding mutations to autism spectrum disorder. *Nature*. 2014;515:216–221, doi:10.1038/nature13908.
39. Sun W, Huang L, Xu Y, et al. Exome sequencing on 298 probands with early-onset high myopia: approximately one-fourth show potential pathogenic mutations in RetNet genes. *Invest Ophthalmol Vis Sci*. 2015;56:8365–8372, doi:10.1167/iovs.15-17555.
40. Marmor MF, Fulton A, Holder G, et al. ISCEV Standard for full-field clinical electroretinography (2008 update). *Doc Ophthalmol*. 2009;118:69–77.
41. McCulloch DL, Marmor MF, Brigell MG, et al. ISCEV Standard for full-field clinical electroretinography (2015 update). *Doc Ophthalmol*. 2015;130:1–12.
42. Richards S, Aziz N, Bale S, et al. Standards and guidelines for the interpretation of sequence variants: a joint consensus recommendation of the American College of Medical Genetics and Genomics and the Association for Molecular Pathology. *Genet Med*. 2015;17:405–424, doi:10.1038/gim.2015.30.
43. Kopanos C, Tsiolkas V, Kouris A, Chapple CE, Albarca Aguilera M, Meyer R, et al. VarSome: the human genomic variant search engine. *Bioinformatics*. 2019;35:1978–19680, https://doi.org/10.1093/bioinformatics/bty897.
44. Arepalli S, Srivastava SK, Hu M, Kaiser PM, Dukles N, Reese JL, et al. Assessment of inner and outer retinal layer metrics on the Cirrus HD-OCT Platform in normal eyes. *PLoS One*. 2018:13:e0203324, https://doi.org/10.1371/journal.pone.0203324.
45. Ramamurthy V, Niemi GA, Reh TA, Hurley JB. Leber congenital amaurosis linked to AIPL1: a mouse model reveals destabilization of cGMP phosphodiesterase. *Proc Natl Acad Sci USA*. 2004;101:13897–13902, doi:10.1073/pnas.0404197101.
46. Cheguru P, Majumder A, Artemyev NO. Distinct patterns of compartmentalization and proteolytic stability of PDE6C mutants linked to achromatopsia. *Mol Cell Neurosci*. 2015;64:1–8, doi:10.1016/j.mcn.2014.10.007.
47. Grau T, Artemyev NO, Rosenberg T, et al. Decreased catalytic activity and altered activation properties of PDE6C mutants associated with autosomal recessive achromatopsia. *Hum Mol Genet*. 2011;20:719–730, doi:10.1093/hmg/ddq517.
48. Zobor D, Zobor G, Kohl S. Achromatopsia: on the doorstep of a possible therapy. *Ophthalmic Res*. 2015;54:103–108, doi:10.1159/000435957.
49. Thiadens AA, Somervuo V, van den Born LI, et al. Progressive loss of cones in achromatopsia: an imaging study using spectral-domain optical coherence tomography. *Invest Ophthalmol Vis Sci*. 2010;51:5952–5957.
50. Thomas MG, McLean RJ, Kohl S, Sheth V, Gottlob I. Early signs of longitudinal progressive cone photoreceptor degeneration in achromatopsia. *Br J Ophthalmol*. 2012;96:1232–1236, doi:10.1136/bjophthalmol-2012-301737.
51. Genead MA, Fishman GA, Rha J, et al. Photoreceptor structure and function in patients with congenital achromatopsia. *Invest Ophthalmol Vis Sci*. 2011;52:7298–7308, Published 2011 Sep 21, doi:10.1167/iovs.11-7762.
52. Sundaram V, Wilde C, Aboshiha J, et al. Retinal structure and function in achromatopsia: implications for gene therapy. *Ophthalmology*. 2014;121:234–245, doi:10.1016/j.ophtha.2013.08.017.
53. Sadowski B, Zrenner E. Cone and rod function in cone degenerations. *Vision Res*. 1997;37:2303–2314, doi:10.1016/s0042-6989(97)00025-4.
54. Khan NW, Wissinger B, Kohl S, Sieving PA. CNGB3 achromatopsia with progressive loss of residual cone function and impaired rod-mediated function. *Invest Ophthalmol Vis Sci*. 2007;48:3864–3871.

Investigative Ophthalmology & Visual Science